RCS approach for Identifying Metallic Objects in Soil in Order to Detect UXOs

Christian Siebauer*, Heyno Garbe
Institute of Electrical Engineering and measurement Technology, Leibniz University Hannover, Germany

Abstract

As a result of the First and Second World War, many areas of former battlefields are littered with non-detonated explosive devices. Therefore, the disposal of these hazards has been intensively pursued for decades. Unfortunately, it often turns out to be difficult to differentiate between non-detonated bombs, which can be buried to 10 m deep in the ground, and non-hazardous metallic objects. In this paper a reconstruction method is discussed, which combines the borehole inspection with a radar cross-section analysis to facilitate a better identification of the buried object.

1 Introduction

As described in previous papers [1] that in the course of World War II, an extreme number of 2.7 million tons of bombs had been dropped over Europe. By experience about 10 % of these didn't explode when they hit the ground [2]. It can be concluded that up to 270000 tons of non-detonated bombs can still be found under the surface up to a depth of 10 m and present a potential thread especially in the construction industry. In order to overcome that problematic several units have been formed for ground investigations and to detect, unearth and dispose these buried unexploded ordnance (UXO) e.g. the Explosive Ordnance Disposal Service in Germany. The soil represents a disturbed EM environment as it exists for typical EMC measurements. Nowadays, many different measurement techniques are available depending on the surrounding condition, type of UXO and depth is presumed.

A commonly used method for metallic UXO, which are several meters under ground, is the magnetic borehole inspection. Under this procedure, several boreholes are drilled in a specific pattern around the suspicion point and plastic tubes inserted [2]. An example for a drill pattern is given in Fig. 1. By means of a magnetic probe, the Earth's magnetic field is measured along the tubes. Since ferromagnetic materials distort the Earth's magnetic field in their surrounding a spatially limited change of the magnetic field indicates a ferromagnetic object in the near of the probe. By involving the probe data of multiple boreholes, the position and size of a buried object can be estimated. However, an estimation of the geometry is not possible or only to a very limited extent. This problem leads to unnecessary salvage of non-hazardous metallic objects that are due to the measurement data mistakenly considered as UXO.

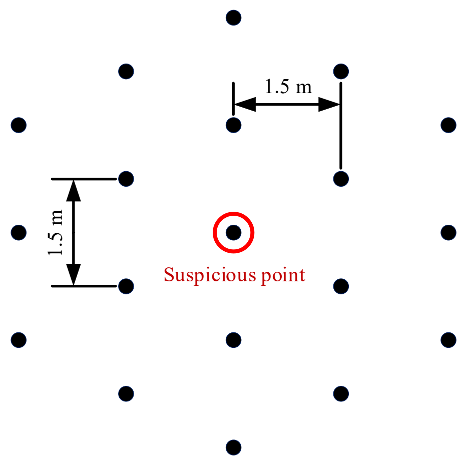

Figure 1. Example for Borehole Pattern [2]

In [1], considerations and simulations for two reconstruction methods were carried out, which should enable better identification of the buried object. With the help of a borehole ground penetrating radar (BH GPR) and the position data from the magnetic borehole inspection, an evaluation of the echo propagation times (Travel Time Method) and signal strengths (Intensity Method) is made. In this work, the focus is on the latter reconstruction method. Hereby the objects geometry should be interpreted similar to the evaluation of the radar cross section (RCS).

2 Simulation Setup

The aim of the simulation setup is to reproduce a BH GBR measuring system in boreholes according to the borehole pattern in Fig. 1. The simulation software used for this examination is gprMax [3]. This software is open source and designed for ground penetrating radar. Although this paper deals with homogeneous soil, this tool can also be used to model more complex soil structures.

The dimensions of the simulation volume are $8\text{ m} \times 8\text{ m} \times 3.2\text{ m}$, which is discretized in cubes of $1\text{ cm} \times 1\text{ cm} \times 1\text{ cm}$. The simulation medium is based on dry sandy soil with a relative permittivity of $\varepsilon_r = 6$ and a loss angle $\tan\delta = 0.0036$. A layer of air with 20 cm height is inserted at the upper limit of the simulation room. The DUT shown in Fig. 2 has a length of 76 cm with a diameter of 21 cm and is horizontal centered in a depth of 1.5 m beneath the air layer. PEC was chosen as the material for the DUT.

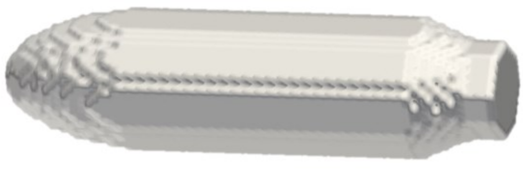

Figure 2. Simulated DUT

The boreholes are arranged as shown in Fig 1, with the pattern shifted horizontally by 50 cm in the x and y directions to avoid a borehole running directly through the DUT. The feed antenna is a Hertzian dipole in vertical alignment which can be varied in depth for all boreholes. The echo is evaluated using a field probe located 10 cm below the feed antenna. As feed signal, a Ricker wavelet with a center frequency of 400 MHz is used.

3 Reconstruction Method

The method used for reconstruction is based on the Radar Cross Section (RCS) of the object. The RCS is the characteristic echo of an object depending on its geometry, its orientation and the used wavelength. There are several different mechanisms which produce the resulting RCS [4] with the mechanism of specular scattering and scattering at singularities being of particular importance in the following consideration. The RCS σ is defined as follows

$$\sigma = \lim_{R\to\infty} 4\pi \cdot R^2 \cdot \frac{|E_s|^2}{|E_0|^2} \tag{1}$$

with E_s as the electric field strength of the scattered field received at the antenna, E_0 as the electric field strength of the emitted field to the object and R as the distance between object and antenna. Since this formula assumes wave propagation in air and therefore does not take losses in the medium into account, it cannot be differentiated whether a low RCS value was caused by a small body surface or by the damping losses. Therefore, the formula for this area of application has been modified.

$$\sigma = (2R)^a \cdot \frac{\int |E_s(t)|^2\, dt}{\int |E_{fc}(t)|^2\, dt} \tag{2}$$

The upper integral describes the energy of the received echo signal $E_s(t)$. The lower one describes the energy of a predicted signal $E_{fc}(t)$ that has traveled the distance $2R$ like the echo. The constant a is used to ensure that the RCS is actually independent of the antenna distance. It has been shown in the simulation evaluation that a value less than 2 leads to better results.

3.1 Determination of the wave number k

In order to make a prediction of the unscattered time signal $E_{fc}(t)$, the propagation properties of the soil, represented by the wavenumber k, are required. For this purpose, two reference measurements are carried out at the same depth but at different distances, whereby the simplification is required that the soil is approximately horizontally homogeneous. In the simulation model, the DUT was removed for the reference measurements. In real measurements, the echo would have to be cleaned from the influence of unwanted scatter signals by a suitable choice of the boreholes and different filters. The formula for the electrical far field of a $\lambda/2$ dipole [5] is required to calculate the soil properties.

$$E_\theta = \frac{-jc_0\mu_0 I_0}{2\pi r \cdot \sin\theta} \cos\left(\frac{\pi}{2} cos\,\theta\right) \exp(jkr - j\omega t) \tag{3}$$

The parameter I_0 is the antenna current, c_0 is the speed of light and θ is the polar angle. Since the evaluation of the reference signal takes place at the same height as the feed antenna, it follows that $\theta = \pi/2$. In the next step all constant sizes are summarized to the constant A.

$$E_\theta(r,\omega,t) = \frac{A}{r} \cdot \exp(jk(\omega)r) \cdot \exp(-j\omega t) \tag{4}$$

By forming the ratio of the reference measurements from different distances it follows.

$$\frac{E_1(r_1,\omega)}{E_2(r_2,\omega)} = \frac{\exp(k(\omega)\cdot r_2)}{\exp(k(\omega)\cdot r_1)} \tag{5}$$

$$k(\omega) = \frac{1}{j(r_2 - r_1)} \cdot \ln\frac{E_1(\omega)\cdot r_1}{E_2(\omega)\cdot r_2} \tag{6}$$

Since the spectra E_1 and E_2 are complex quantities, the natural logarithm has no explicit result. Instead, the imaginary part of the logarithm can be a multiple of 2π larger or smaller. As a result, the real part of $k(\omega)$ can be a multiple of $2\pi \cdot (r_2 - r_1)^{-1}$. With this information and the conditions that the imaginary part has to be continuous, it will start around zero for $\omega = 0$ and a rough estimation with the formula,

$$k \approx \omega \cdot \sqrt{\varepsilon\mu} \tag{7}$$

the real part of the wave number can be reconstructed. In the next step, the spectrum E_{fc} can be predicted from the wavenumber k and one of the two reference measurements for any distance from the transmitting antenna.

$$E_{fc}(\omega) = \frac{r_1}{r_{fc}} E_1(\omega) \cdot \exp\left(-jk(\omega)\cdot(r_{fc} - r_1)\right) \tag{8}$$

The time signal $u_{fc}(t)$ can finally be calculated using an inverse Fourier transformation.

3.2 Prediction of the Geometry

The basic idea of this reconstruction method is that each RCS value is assigned to an object geometry area. High

RCS values indicate a large area. If possible, a closed contour should be created by evaluating the DUT from different directions. Since the evaluation is two-dimensional with this method, each RCS value is assigned in a straight line. The direction of this line is determined by the relative angle φ_{rel} between the DUT and the respective measuring point. The contour vector calculates as follows:

$$\vec{v}_{\mathrm{outline}}(n) = \sigma(n) \begin{pmatrix} \cos(\varphi_{\mathrm{rel}}(n)) \\ \sin(\varphi_{\mathrm{rel}}(n)) \end{pmatrix} \tag{9}$$

The procedure described above is shown exemplary in Fig. 3. The blue, yellow and red lines on the right side represents the RCS strength from the respective radiation direction. The left side shows the reconstructed contour of the body by adding up the outline vectors from formula (9).

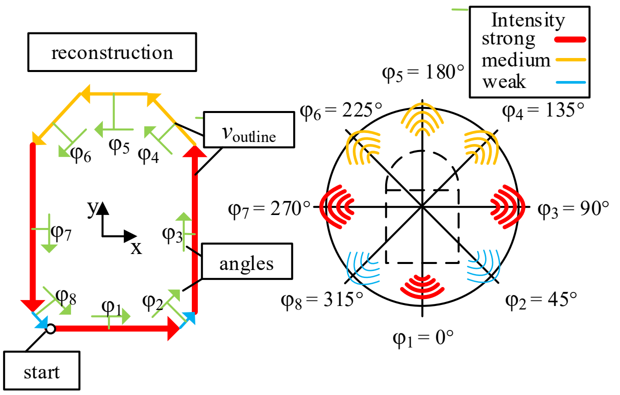

Figure 3. Representation of RCS reconstruction method

4 Results

In the first step, the simulated reference signals were filtered and cleaned of unwanted echoes, such as reflections at the surface-air transition. Fig. 4 shows the reference signals for a depth of 1.5 m.

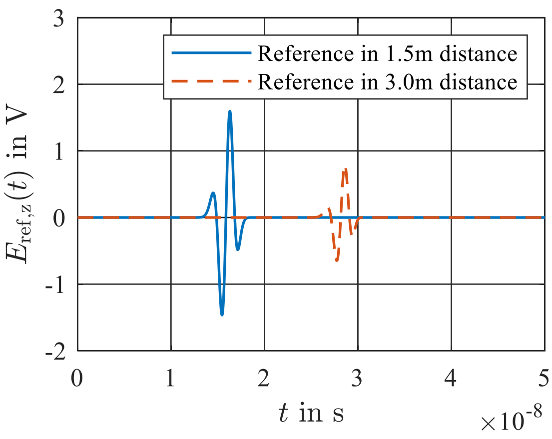

Figure 4. Reference Signals in a depth of 1.5 m

Formula (6) was used to calculate the wavenumber k which was then corrected in the real part. Corrected and uncorrected Real part of the wavenumber is shown in Fig. 5.

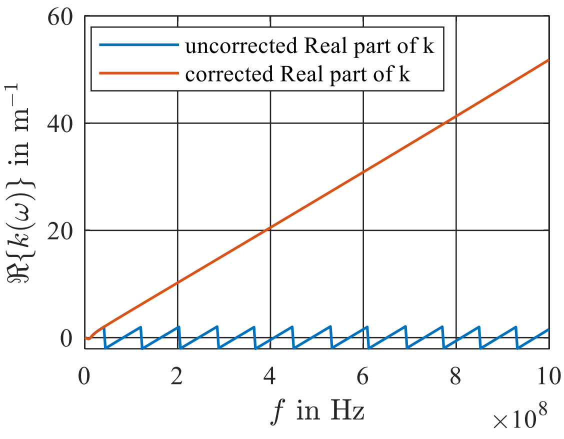

Figure 5. Real Part of calculated Wavenumber k

In the next step, the time that corresponds to the shortest distance between the borehole and the DUT is determined from the simulation results for each borehole position. Fig. 6 shows the absolute value of the received field for one borehole. The white marked point is used for further calculation of the predicted signal.

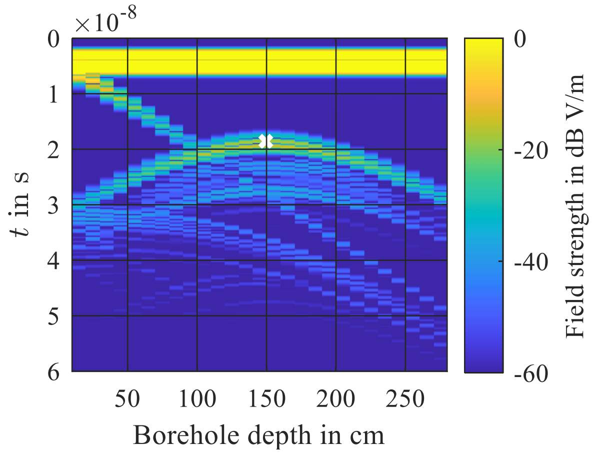

Figure 6. Absolute value of received field data

The speed of the electromagnetic wave in the ground is required to convert selected transit times into corresponding distances $2R$. The reference measurements can be used again for this. The integral limits in (2) are chosen so that only the expected signal width is included. Although a calculation with the power $a = 2$ already leads to good results, a power of $a = 1.44$ was chosen for the following evaluation. This size was determined by simulating an ideal sphere, since it can be assumed that the RCS in this case must be constant over the angle φ and distance R. The determined RCS values are next sorted in ascending order according to the angle and then interpolated to obtain a constant step size. Due to the chosen power a, a unit for the graphical representation of the estimated DUT contour should be omitted here. Fig. 7 shows the reconstruction of the DUT using the method described (solid line). Since a closed contour cannot be achieved with the evaluation of the RCS, an example of a possible closed contour was also shown (dashed line). This was achieved by fulfilling the condition that the start and end point must be on top of each other. The resulting displacement vector was applied to the neighboring points in a linearly decreasing manner. With the information that flat surfaces lead to a strongly increased echo, it becomes clear why the flat side of the DUT on the right side in Fig. 7 is more distinctive than the actual geometry in Fig. 2 indicates. However, the elongated shape of the body with the ellipsoid tip at the left end is clearly visible.

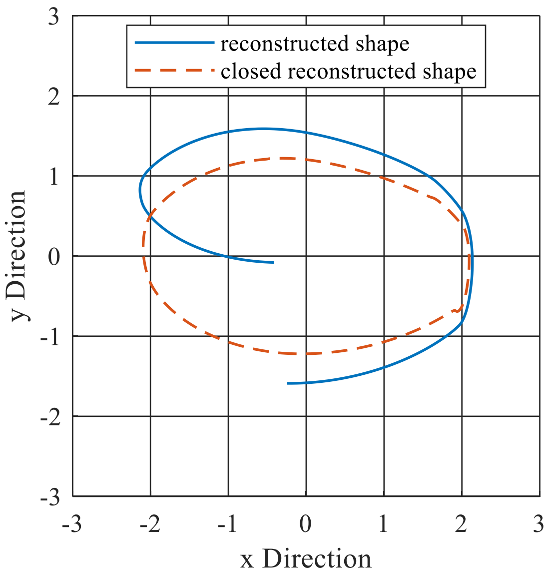

Figure 7. Reconstruction of the DUT

For the purpose of comparability, Fig. 8 shows the RCS of the ideal sphere mentioned previously, which was used to determine the constant a. This has a diameter of 10 cm and was placed analog to the DUT.

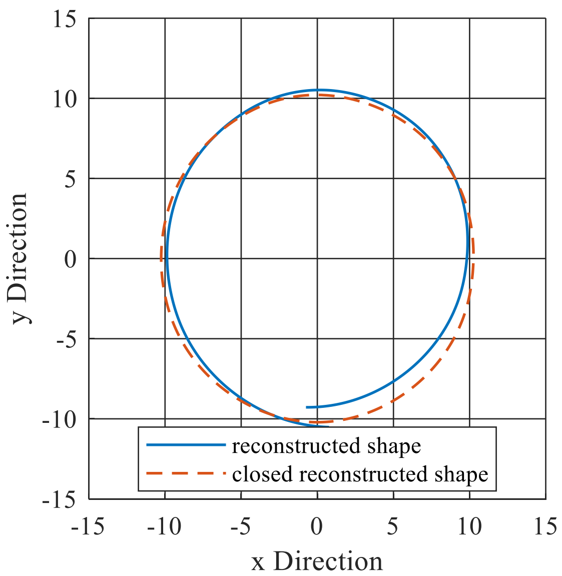

Figure 8. Reconstruction of ideal sphere

5 Summary

In the removal of buried unexploded Ordnance (UXO), not only the detection but also the identification of these metallic anomalies is a great challenge. This leads to the avoidable salvage of harmless metallic objects. In this paper a reconstruction method is presented which can be carried out after a magnetic borehole inspection and which should enable a better identification of the buried object. For this purpose, the already made measuring boreholes are used to carry out further measurements with an electromagnetic borehole radar system. The method is based on an evaluation of the radar cross section (RCS) and aims at an evaluation of the object geometry in accordance with its reflection property. The difficult to handle measuring environment of the soil and its damping effect must be taken into account in the calculation by reference measurements. The presented simulation results show that with the help of the reconstructed envelope, conclusions can be drawn about the real object geometry. The next step is to carry out a proof of concept in a real environment.

6 Acknowledgements

The author would like to thank Dirk Sonnemann (Hannover Fire Department), as well as Dr. Michael Horn (Schollenberger Kampfmittelbergung GmbH).

7 References

[1] C. Siebauer, M. Terres and H. Garbe, "Identification of Metallic Object in Soil in Order to Detect UXOs," in *2019 International Symposium on Electromagnetic Compatibility - EMC EUROPE*, Barcelona, Spain, 2019.
doi: 10.1109/EMCEurope.2019.8871972

[2] Oberfinanzdirektion Niedersachsen, „Arbeitshilfen Kampfmittelräumung Leitstelle des Bundes für Kampfmittelräumung," Bundesministerium für Umwelt, Naturschutz, Bau und Reaktorsicherheit (BMUB), 2014.

[3] C. Warren, A. Giannopoulos and I. Giannakis, "gprMax: Open source software to simulate electromagnetic wave propagation for Ground Penetrating Radar," *Computer Physics Communications,* pp. 163-170, December 2016.
doi: 10.1016/j.cpc.2016.08.020

[4] M. Skolnik, Radar Handbook, New York: McGraw-Hill, 2008, pp. 14.1-14.4.

[5] M. E. Everett, Near-Surface Applied Geophysics, Texas A & M University: Cambridge University Press, 2013, pp. 265-268.
doi: 10.1017/CBO9781139088435